Gravity signal at Ghawar, Saudi Arabia, from the global gravitational field model EGM 2008 and similarities around

J. Klokočník & J. Kostelecký

Arabian Journal of Geosciences

ISSN 1866-7511

Arab J Geosci
DOI 10.1007/s12517-014-1491-y

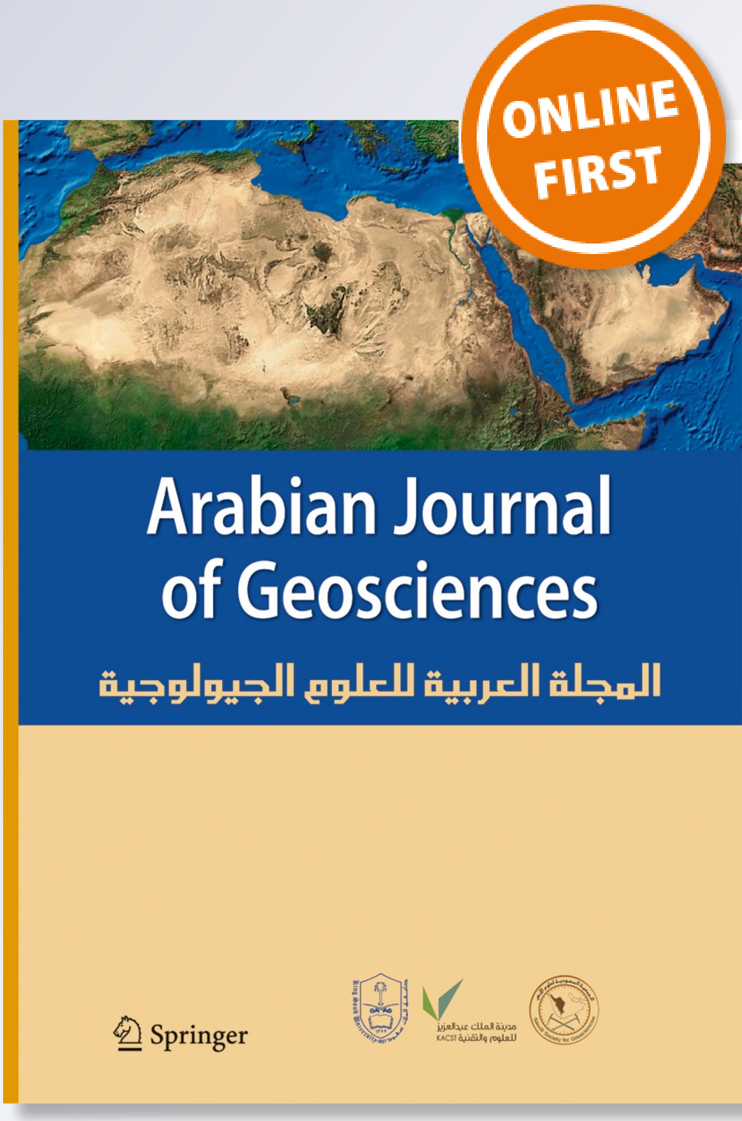

Springer

Arab J Geosci
DOI 10.1007/s12517-014-1491-y

ORIGINAL PAPER

Gravity signal at Ghawar, Saudi Arabia, from the global gravitational field model EGM 2008 and similarities around

J. Klokočník · J. Kostelecký

Received: 6 February 2014 / Accepted: 2 June 2014

Abstract Gravity disturbances (or free-air anomalies), the Marussi tensor, invariants of the gravity field, and other functionals and functions (here called *aspects*) of the geopotential, as represented by recent global gravitational field models, are computed for Ghawar, Saudi Arabia, (Al-Anazi, 2007) (Al-Almazi, 2007) and for surrounding areas. With the free-air gravity anomalies, derived from the Earth Gravitational Field Model 2008 (EGM 2008) or European Improved Gravity model of the Earth by New techniques (EIGEN)-6C3 gravity models (based on satellite as well as terrestrial data), we can see features well known to geologists, geophysicists, geomorphologists, and others. Resolution with the global gravitational models is, however, lower than with terrestrial data only, but our "view" is global. With the invariants, strike angles, and virtual deformations, we can find more interesting features (than with the gravity anomalies themselves). We can see analogies between places with oil deposits in the area of the Caspian Sea, Ghawar in Saudi Arabia, and other localities nearby. It is evident that the only "gravity signal" (the aspects) cannot decide about possible deposits of any mineral or oil but—as is known on a local scales—can be a useful tool, which—in conjunction with other data and experience of specialists—may lead to some discoveries. Several interesting places are indicated by the strike angles and virtual deformations at the Persian and Oman Gulfs, Saudi Arabia, the United Arab Emirates (UAE) and the Red Sea.

Keywords Gravity disturbance (anomaly) · Marussi tensor · Invariants of the gravity field · Strike angles · Virtual deformations · The Earth Gravitational Model 2008 · Ghawar

Introduction

Global combined gravitational field models of the Earth (sets of harmonic geopotential coefficients, also known as Stokes parameters), determined to high degree and order harmonic expansion of the geopotential, from various satellite and terrestrial data, can today have worldwide high resolution and precision. The Earth Gravitational Field Model 2008 (EGM 2008, Pavlis et al. 2008a, b, 2012) uses multiyear inter-satellite range-rate data from a near polar-orbiting tandem of satellites called Gravity Recovery and Climate Experiment (GRACE) together with extensive gravity anomalies derived from terrestrial gravimeters and satellite altimetry. EGM 2008 reaches a resolution of 5×5 arcmin, which is ~9 km of half wavelength on the Earth's surface at the equator (about 8 km at Saudi Arabia), and, with the exception of Antarctica and some others areas, mostly mountain belts, a precision of free-air anomalies, derived from the potential of EGM 2008, is of the order few miliGals. Where EGM 2008 lacks adequate precision and resolution, topographic data from satellites serve as the "fill-in data" (see more about it in Pavlis et al. 2012). The new data coming from the gradiometer on board of Gravity Field and Steady-State Ocean Circulation Explorer (GOCE, ESA mission, e.g., Floberghagen et al. 2011) were already implemented into the newest gravitational models, e.g., to a combined model European Improved Gravity model of the Earth by New techniques (EIGEN)-6C3 (Förste et al.

J. Klokočník (✉)
Astronomical Institute, Academy of Sciences of the Czech Republic, 251 65 Ondřejov, Fričova 298, Czech Republic
e-mail: jklokocn@asu.cas.cz

J. Klokočník
e-mail: bezdek@asu.cas.cz

J. Kostelecký
Research Institute of Geodesy, Topography and Cartography, 250 66 Zdiby 98, Czech Republic
e-mail: kost@fsv.cvut.cz

Published online: 26 June 2014

2013), providing precision and resolution comparable to EGM 2008.

Such gravitational field models offer new opportunities to many applications in geodesy, geophysics, geology, geomorphology, and physical geography. In this paper, using the harmonic geopotential coefficients of EGM 2008 or EIGEN-6C3, the following physical quantities are computed: the gravity anomalies Δg (or disturbances) [scale 1 mGal= 10^{-5} ms^{-2}], the full Marussi tensor $\mathbf{\Gamma}$ of the second derivatives of the disturbing potential [1E=1 Eötvös=10^{-9} s^{-2}], namely its radial component Γ_{33} (sometimes denoted T_{zz} or T_{rr}), the invariants of the gravity field I_0, I_1, I_2=det ($\mathbf{\Gamma}$), computable from the components of the Marussi tensor, their specific ratio I, and the strike angle θ. These quantities are known from theory of Pedersen and Rasmussen (1990) and Beiki and Pedersen (2010). A "virtual deformation" has been added (Kalvoda et al. 2013). Some of these quantities are functionals of the geopotential in a mathematical sense and some of them are not. Therefore, they are concisely designated in the paper as *aspects* of the geopotential.

The second-order derivatives and the invariants provide evidence about details of near-surface (not deep) structures. The Marussi tensor was already used in local scales (a few kilometers) for petroleum, metal, diamond, groundwater, etc. explorations (e.g., Murphy and Dickinson 2009; Mataragio and Kieley 2009). The full Marussi tensor is a richer source of information than standard single gravity anomalies. This extra information can be applied by tensor imaging techniques to enhance a target anomaly definition, as tested for local features (minerals, oil, and gas industry), e.g., by Saad (2006) or Dickinson et al. (2009).

Theoretical and experimental studies mentioned above were our stimulation to examine larger regions—in other words, to advance from local scales to the global gravitational models. Previously, the gravity anomalies or the second derivatives were derived from measurements by gravimeters on the ground, airplanes, or ships or by gradiometers on airplanes. For the first time, we compute the aspects listed above, based on a new global gravitational field model. The local scale (~1 km) is below the resolution of the EGM 2008. Tests of the sensitivity of the aspects of the EGM 2008 to selected landform patterns were realized by Klokočník et al. (2010) using especially large impact craters and by Kalvoda et al. (2010) in Himalayan regions with very conspicuous relief features of active orogeny and intensive climate-morphogenetic processes.

Previous experience leads us to investigate also areas with oil deposits. We discovered unexpected behavior of the strike angles and the virtual deformations in a "belt" crossing the Caspian Sea. We also can "see" Ghawar in Saudi Arabia with the EGM 2008. It was inspiring to extrapolate and to test whether other localities nearby may show similar features. Examples are stated in "Results and discussions." We are fully aware that this research cannot result in deposit predictions without analyzing other necessary data and we—as geodesists—cannot provide them, but this research possibly can stimulate other specialists to continue.

Notes to theory and data

All definitions needed and formulae used in our software are described in Kalvoda et al. (2013) and will not be repeated here. *Gravity anomaly* is a radial derivative of the disturbing potential. The gravity gradient tensor $\mathbf{\Gamma}$ (the *Marussi tensor*) is a tensor of the second derivatives of the disturbing potential. The horizontal components of the tensor help to identify the shape and geological setting of a target body. The vertical component Γ_{33} is best suited for target body detection; Γ_{33} helps to define isopath/density relationships of a body mass with relation to its geological setting (e.g., Murphy and Dickinson 2009). Under any coordinate transformation, $\mathbf{\Gamma}$ preserves just three *invariants* of the gravity field, nonlinear combinations of the components of the Marussi tensor. Pedersen and Rasmussen (1990) showed that a *specific ratio of the two invariants* lies between 0 and unity for any potential field. If the causative body is strictly 2D, then this ratio equals 0. The *strike angle* θ_S is another nonlinear combination of the components of the Marussi tensor. The strike angle indicates how gradiometer measurements rotate within the main directions of the underground structures. For more details, see Pedersen and Rasmussen (1990) and Beiki and Pedersen (2010).

To define the term "*virtual deformation*," we utilized an analogy with the tidal deformation, and applying the apparatus of mechanics of continuum, we derived the main directions of the tension. Explanation is again stated in Kalvoda et al. (2013); we plot the main directions of possible deformations. The virtual deformations are geometrically expressed by its dilatation or compression. Virtual dilatations of deformation indicate uplifted regions at the geoid, a mass of which has tendency to disintegration; the virtual compressions indicate lowered zones at the geoid. Natural processes, which are the cause of these states of the near-surface part of the geoid, are very diverse and are not discussed here.

Our data basis consists of the harmonic geopotential coefficients of the global gravitational field models mentioned above (EGM 2008 or EIGEN-6C3). The *terrestrial data* base of EGM 2008 is very extensive and consists of several sources—gravimetric measurements, anomalies derived from altimetry, and fill-in data from digital models of the terrain relief when nothing better was available, see Pavlis et al. (2012). EGM 2008 is still probably the best currently available combined gravitational field model of the Earth.

Plotting is important for visualizing our results; we make use of strongly nonlinear scales to emphasize various features which otherwise might remain hidden. A note about the units of plotted functionals, mGal for the gravity anomalies and/or disturbances, E=Eötvös for the second order potential derivatives. The invariants I_1 and I_2 have units [s^{-4}] and [s^{-6}], and their ratio I is spaceless. The strike angle θ_S is expressed in degrees, and its demonstration in red means its direction to the east and in blue to the west of the local meridian. The virtual deformations are dimensionless and express a direction of dilatation (red) or compression (blue). These units are used in all figures presented below.

Results and discussions

A systematic worldwide screening of the aspects has been performed (Kalvoda et al 2013; Klokočník et al. 2012, 2013;

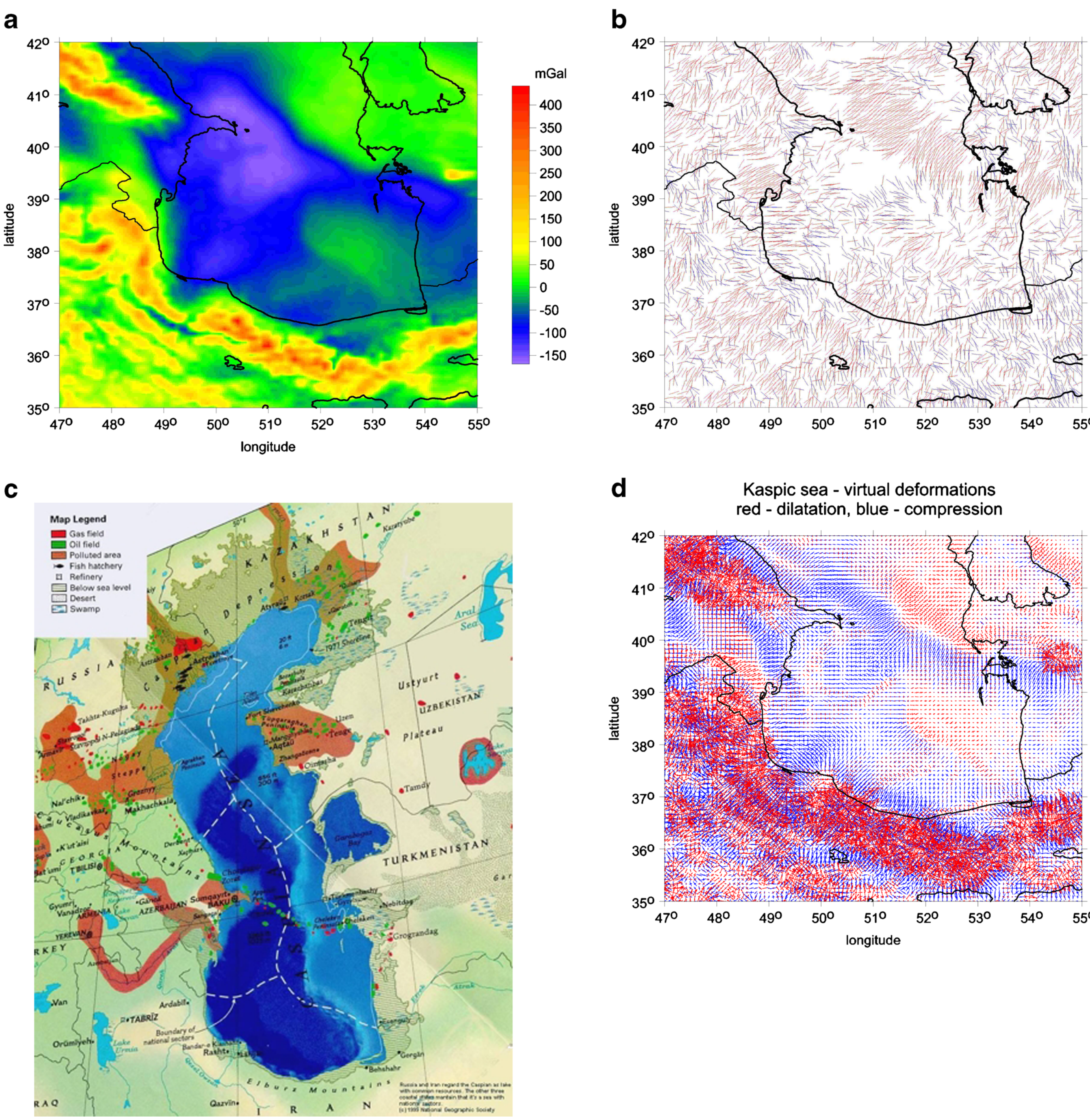

Fig. 1 **a** Southern parts of the Caspian Sea and its neighboring areas, Δg. **b** The strike angle for the ratio $I< 0.3$. Note the belt of vectors oriented to one side, crossing the central part of the Caspian Sea. **c** A map of oil and gas fields in the Caspian Sea area. A *green* "belt" crosses the Sea roughly in west-east direction. **d** The virtual deformations (*red* is dilatation and *blue* compression of the ellipse of deformation). See the "belt" going roughly from northwest to southeast across the Caspian Sea

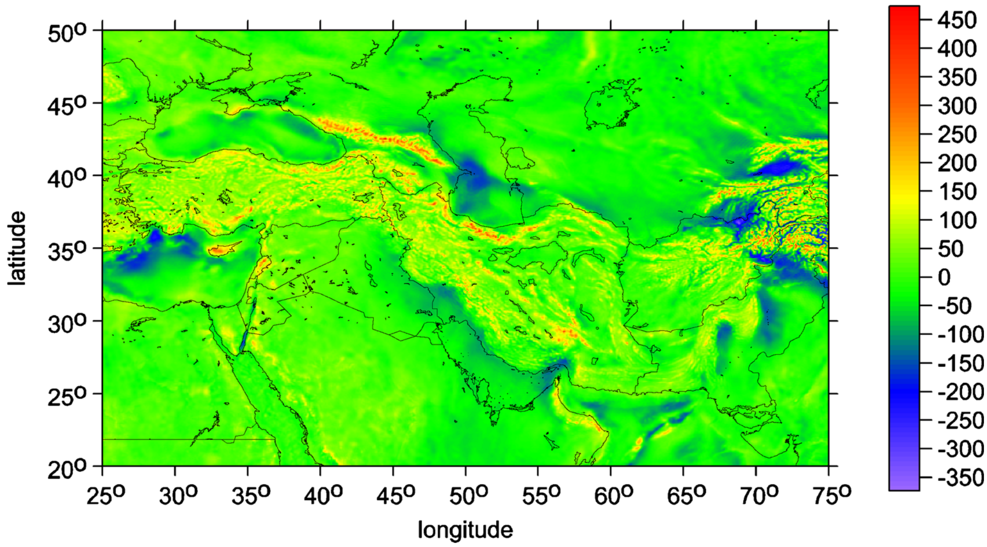

Fig. 2 The Caspian Sea, Turkey, Iran, Iraq, Afganistan, Pakistan, Turkmenistan, Israel, Syria, Jordan, Kuwait, the Persian Gulf, the Zagros Mts., Saudi Arabia, Qatar, UAE, Oman, a part of the Red Sea, a general look of the gravity disturbancies Δg (scale in miliGal)

www.asu.cas.cz/~jklokocn). Here, we focus on the Caspian Sea, Ghawar area in Saudi Arabia, and surrounding areas with similar "gravity signal."

It was inspiring to see the strong negative gravity disturbancies (Fig. 1a) and the strike angle values (Fig. 1b) crossing the Caspian Sea. We compared to a map of oil and gas field in that area (Fig. 1c) and to the virtual deformations, showing systematic patterns of dilatation and compressing crossing the sea (Fig. 1d); one is then asking what it may mean? Such "combed" patterns of the strike angles and deformations in huge scales are not too frequent. According to theory of Pedersen and Rasmussen (1990) and Beiki and Pedersen (2010), the strike angles for small values of the ratio I indicate areas with flat (like 2D) causative bodies which here might be valid for oil deposits. A figure showing the same for $I > 0.3$ would be complementary to Fig. 1b.

As an introduction to the area of our interest, we show gravity disturbancies in the large region of the Caspian Sea, Afghanistan, Persian Gulf, Iranian Highland, Zagros Mts., Saudi Arabia, and others (Fig. 2); one example from our work is the work of Kalvoda et al. (2013). Then, we zoom in individual regions in series of figures (Fig. 3a–n). The main patterns of the strike angles θ_S (Fig. 3a) in the section between the Iranian Highland, the Zagros Mts., the Persian Gulf, and part of Saudi Arabia are manifested. On the contrary, Fig. 3b–f shows the values of the aspects in "relatively small" area of the Ghawar oil fields in Saudi Arabia (~100 km long in a south-north direction). Conspicuous harmony between a course of zones with positive values of Γ_{33} (Fig. 3b) and virtual dilatations of the ellipse of deformation (Fig. 3f) testifies in favor of the existence of matter elevation situated in a nearly meridian direction. This elevation is surrounded on the western and eastern sides by zones of negative values of Γ_{33} and/or virtual compressions of the ellipse of deformation, which can be interpreted as a manifestation of linear near-surface depressions. The described situation is supported by an occurrence of stripes of I_2, I, and θ_S (Fig. 3c–f).

Back to Fig. 3a with the strike angles, we see several localities, including Ghawar, where the angles are oriented dominantly in one direction; in other places, they are chaotic. We will confront this with the virtual deformations. Figure 3f shows them for the Ghawar large oil fields. Figure 3g–i is for a larger area (as in Fig. 3a). In Fig. 3f, the virtual deformations create three belts in west-east direction, "central" belt of dilation surrounded by two belts of compression with similar orientation as the strike angles, which are depicted in Fig. 3e.

We split dilatation and compression and show them in two separate figures. While Fig. 3g shows all the virtual deformations together, Fig. 3h shows only the dilatation and Fig. 3i only the compression. Note that in areas encircled in Fig. 3a, there is remarkable agreement between the strike angles and the deformations. The area 1 (Ghawar) and the areas in Irán are shown as oil and gas fields (Pollastro et al. 1997). The compressive part of the deformations (Fig. 3i) also shows correlations with topographic features of circular-like type

Fig. 3 **a** The strike angle for $I < 0.3$ for a part of Iran, the Persian Gulf, Saudi Arabia, UAE, Oman, part of the Red Sea. Note several zones with the angles oriented dominantly in one direction, see *circles* or *ellipses*. Comments to the *encircled zones* 1–6 are below. **b** The values of Γ_{33} for Ghawar in Saudi Arabia. **c**The invariant I_2. **d** The ratio I of the invariants I_1 and I_2. **e** The strike angle θ_S for the ratio $I < 0.3$, superimposed on a Google Earth map. **f** The virtual deformations (*red* is dilatation and *blue* compression) in the area of the Ghawar oil fields. **g** The virtual deformations (*red* is dilatation and *blue* compression) in Saudi Arabia, Persian Gulf, part of Iran, and other countries. **h** The virtual deformations (only dilatation) in Saudi Arabia, Persian Gulf, part of Iran, and other countries. **i** The virtual deformations (only compression) in Saudi Arabia, Persian Gulf, part of Iran, and other countries. **j** The invariant I_2 (similarly for I_1). **k**, **l** The strike angles (*left*) and virtual deformations for the area "2" (see Fig. 3a), from Iran crossing the Persian Gulf to Quatar. **m**, **n** The strike angles (*left*) and virtual deformations for the area "3" (see Fig. 3a) in the Persian Gulf, Emirates, and Oman ▶

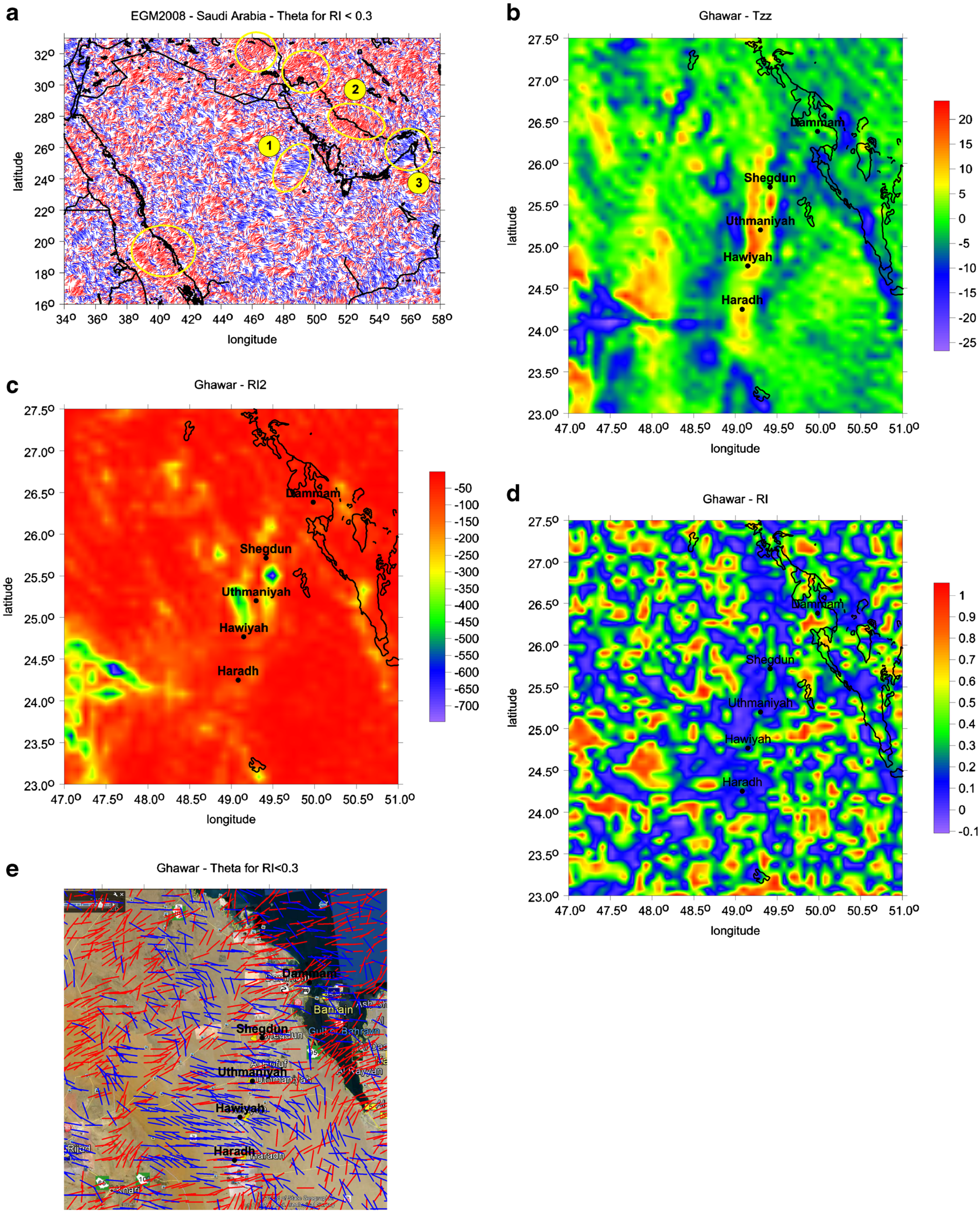

over many places in Saudi Arabia (which reader can verify by using Google Earth satellite images).

The invariants in the same area (as in Fig. 3a) look very "inactive" inside Saudi Arabia (see Fig. 3j) and are (as is

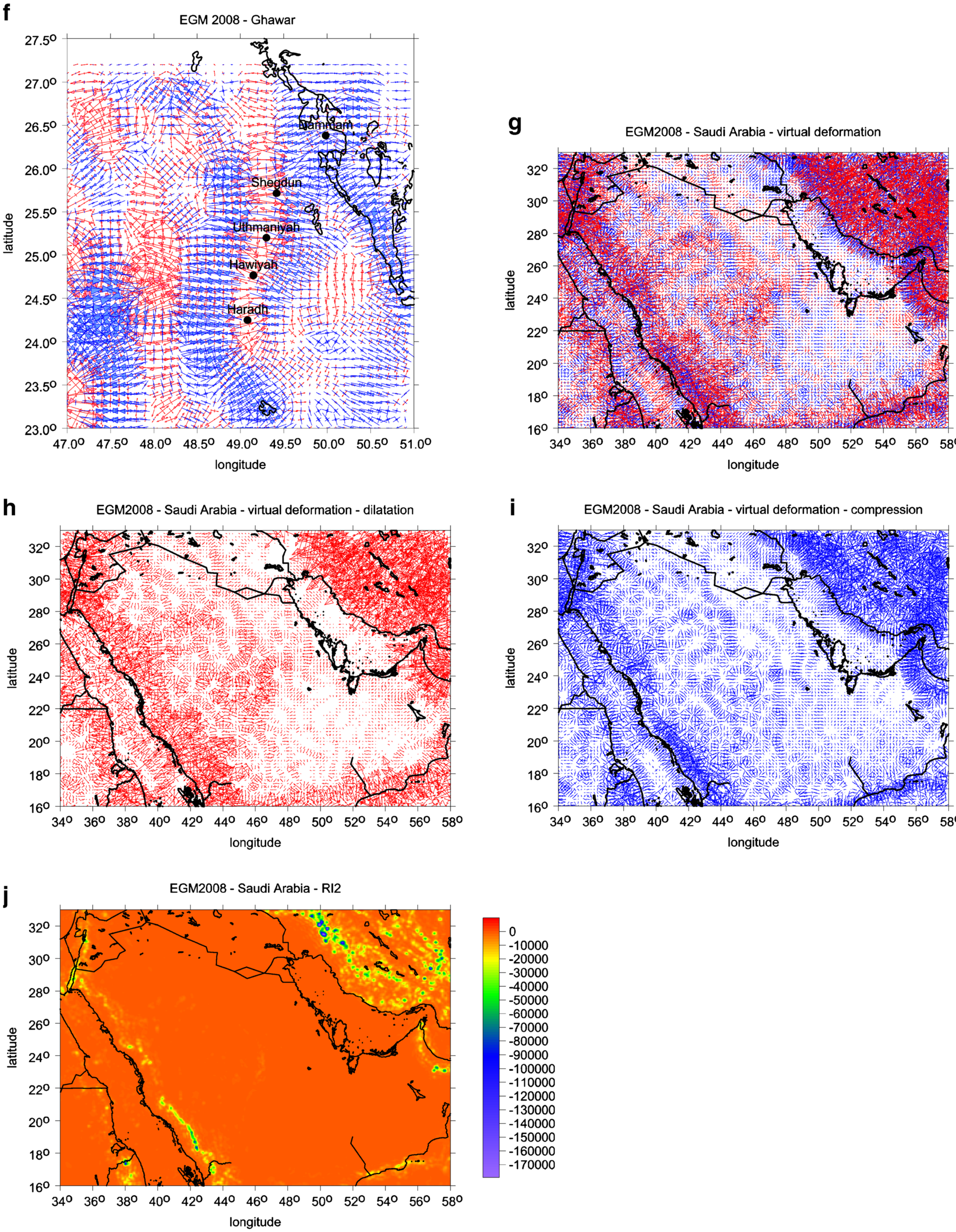

Fig. 3 (continued)

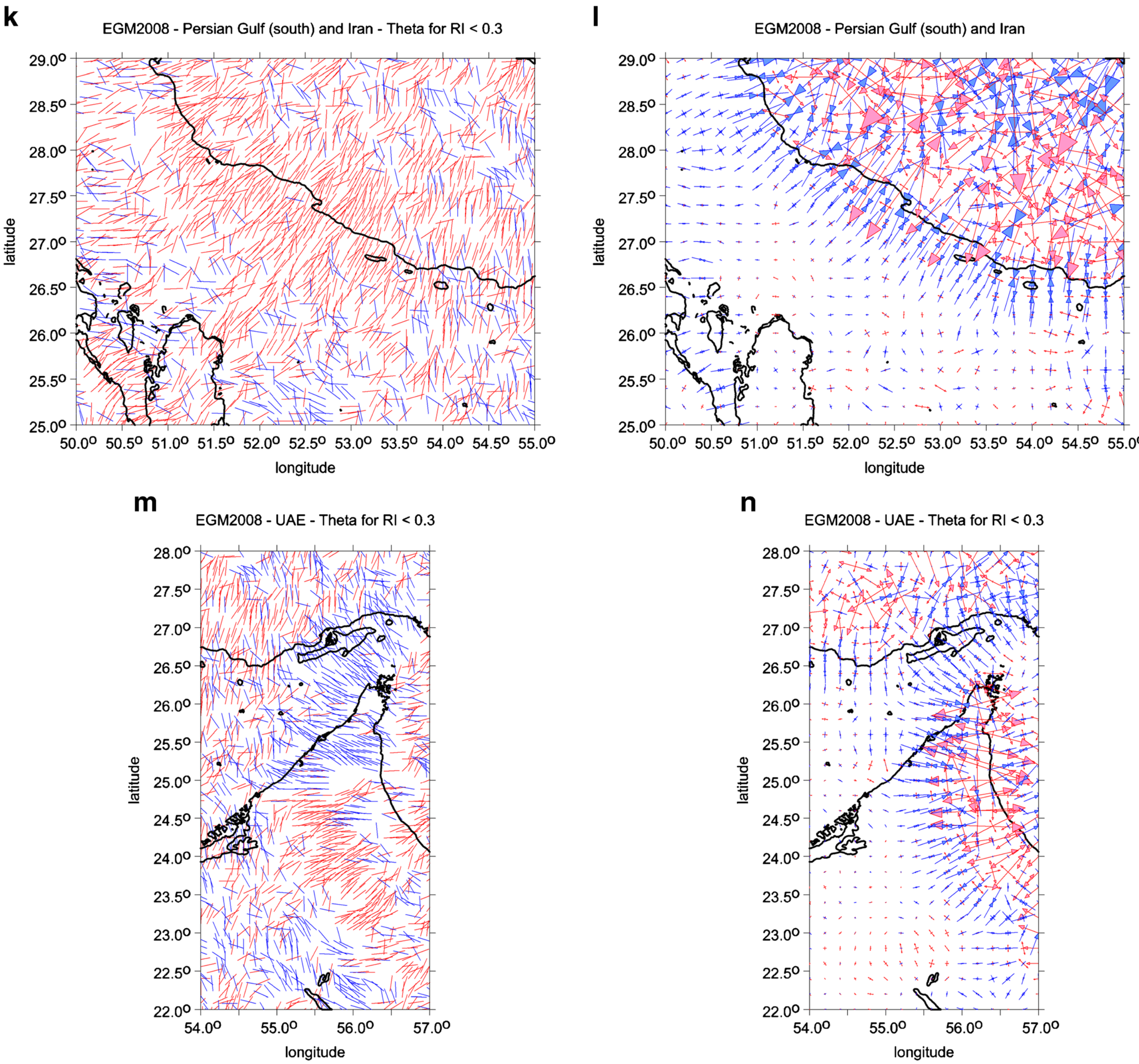

Fig. 3 (continued)

expected and known from various mountain areas or rifts, see Kalvoda et al. 2013) accentuated in the mountain belts.

The encircled zones on Fig. 3a have special figures—zooms with the strike angles and the virtual deformations. For Ghawar, zone “1,” we have Fig. 3e, f. For the area “2” (from Irán crossing the Persian Gulf to Quatar), we show Fig. 3k, l. For the area “3” (between UAE and Oman), we have Fig. 3m, n.

Recalling theory from “Notes to theory and data,” the strike angle indicates main directions of the underground structures, the virtual dilatations indicate uplifted regions of geoid, and the compressions are connected to the lowered zones of geoid. Figure 3k–n clearly shows a correlation between the strike angles and the deformations. Very pronounced is a bent belt of compressions in Fig. 3n.

Conclusions

Theories of Pedersen and Rasmussen (1990) and Beiki and Pedersen (2010) have been extended and applied in various regions of the Earth (Kalvoda et al. 2013), using the global gravitational field model EGM 2008 with a resolution about 10 km on the Earth’s surface (in some areas lower, see Pavlis et al. 2012). For the first time, not local but global or regional views of this type are on offer.

An extensive screening of gravity signatures computed from EGM 2008 (and now also with EIGEN-6C3, not shown here) and their comparison with morphotectonic patterns and orographical features on a large scale was realized (Kalvoda et al. 2013; Klokočník et al. 2010, 2012, 2013). From the methodological and interpretative points of view, it was confirmed that distributions of values of the second derivatives of the disturbing gravitational potential Γ_{33} very precisely represent a near-surface (topographical) mass distribution.

For Saudi Arabia and surrounding countries, we can see interesting patterns of the strike angles and virtual deformations. We show how it looks like at Ghawar, the large oil deposit site. We found analogical gravity signal in a few other localities.

The gravity signal is represented here in the form of various aspects (functions) of the disturbing gravitational potential, but nothing more. Not to leave analysis on this speculative level, we seek for interpreters from geologists or geophysicists to continue our work.

Acknowledgments We thank very much the anonymous reviewer for his helpful and inspiring review. Our work has kindly been supported by grants from the Grant Agency of Czech Republic no. 13-36843S (J. Klokočník) and by the European Regional Development Fund (ERDF), project "NTIS—New Technologies for Information Society," European Centre of Excellence,

NTIS-CZ.1.05/1.1.00/02.0090 (J. Kostelecký).

References

Al-Anazi BD (2007) What you know about the Ghawaroil field, Saudi Arabia*? CSEG Recorder,* April, pp 40–43

Beiki M, Pedersen LB (2010) Eigenvector analysis of gravity gradient tensor to locate geologicbodies. Geophysics 75(6):137–149. doi:10.1190/1.3484098

Dickinson JL, Brewster JR, Robinson JW, Murphy CA (2009) Imaging techniques for full tensor gravity gradiometry data, *11th SAGA BiennalTechn. Meeting & Exhib*., Swaziland, September, pp 84–88

Förste C, Bruinsma S, Abrykosov O, Flechtner F, Dahle C, Neumayer K H, Barthelmes F, König R, Marty J C, Lemoine J M, Biancale R (2013) EIGEN-6C3—the newest high resolution global combined gravity field model based on the 4th releaseofthe GOCE direct approach, *BookofAbstracts*, The IAG ScientificAssembly 2013, 150th Anniv. IAG (Potsdam 2013)

Floberghagen R, Fehringer M, Lamarre D, Muzi D, Frommknecht B, Steiger Ch, Piñeiro J, da Costa A (2011) Mission design, operation and exploitation of the gravity field and steady-state ocean circulation explorer mission. J Geodesy 85:749–758. http://rd.springer.com/article/10.1007/s00190-011-0498-3; http://dx.doi.org/10.1007/s00190-012-0541-z

Kalvoda J, Klokočník J, Kostelecký J (2010) Regional correlation of the Earth Gravitational Model 2008 with morphogenetic patterns of the Nepal Himalaya. Acta Univ Carol Geographica XLV(2):53–78, Prague

Kalvoda J, Klokočník J, Kostelecký J, Bezděk A (2013) Mass distribution of Earth landforms determined by aspects of the geopotential as computed from the global gravity field model EGM 2008. AUC Geographica 48(2):17–25

Klokočník J, Kostelecký J, Pešek I, Novák P, Wagner CA, Sebera J (2010) Candidates formultiple impact craters?: Popigai and Chicxulub as seen by the Global High Resolution Gravitational Field Model EGM08. Solid Earth EGU 1:71–83. doi:10.5194/se-1-71

Klokočník J, Kostelecký J, Kalvoda J, Sebera J, Bezděk A (2012) Towards a system of datasystems in geoscience: Marussi tensor and invariants of the Earth Gravity Field from recent global gravity models EGM 2008 and EIGEN 6C based on satellite (GRACE or GOCE) and terrestrial data – poster, the *Japan Geoscience Union Meeting 2012*, May, Makuhari, Chiba, Tokyo, Japan

Klokočník J, Kalvoda J, Kostelecký J, Bezděk A (2013) Gravity disturbancies, Marussi tensor, invariants and other derivates of the geopotential represented by Global Gravity Field Model EGM 2008 and suggested for geo-applications in various regions of the Earth, *ESA Living Planet Symposium*, September, Edinburgh, Scotland, poster 2–P–228

Mataragio J, Kieley J (2009) Application of full tensor gradient invariants in detection of intrusion-hostedsulphide mineralization: implications for deposition mechanisms. Min Geosci EAGE 1st break 27:95–98

Murphy CA, Dickinson JL (2009) Exploring exploration play models with FTG gravity data, *11th SAGA Biennal Techn. Meeting & Exhib.,* September, Swaziland, pp 89–91

Pavlis NK, Holmes SA, Kenyon SC, Factor JK (2008a) EGM2008: an overview of its development and evaluation, National Geospatial-Intelligence Agency, USA, presented at the interntl.conf.*Gravity, Geoid and Earth Observation 2008*, 23rd–27th June, Chania, Crete, Greece

Pavlis NK, Holmes SA, Kenyon SC, Factor J K (2008b) An earth gravitational model to degree 2160: EGM2008, *EGU General Assembly 2008,* 13–18th April, Vienna, Austria

Pavlis NK, Holmes SA, Kenyon SC, Factor J K (2012) The development and evaluation of the Earth Gravitational Model 2008 (EGM2008). J Geophys Res 17:B04406. doi:10.1029/2011JB008916

Pedersen BD, Rasmussen TM (1990) Thegradient tensor of potential field anomalies: some implications on data collection and data processing of maps. Geophysics 55(12):1558–1566

Pollastro RM, Persits FM, Steinshouer D W (1997) Maps showing geology, oil and gas fields and geologic provinces of Iran, version 1.0, Open-File Report 97/470G, USGS Central Region Energy Resources Team

Saad AH (2006) Understanding gravity gradients—a tutorial, the meter reader, *The Leading Edge,* August, pp 942–950